AIP | Journal of Applied Physics

Magnetocaloric and transport study of poly- and nanocrystalline composite manganites La0.7Ca0.3MnO3/La0.8Sr0.2MnO3

M. Pękała, K. Pękała, V. Drozd, K. Staszkiewicz, J.-F. Fagnard et al.

Citation: J. Appl. Phys. **112**, 023906 (2012); doi: 10.1063/1.4739262
View online: http://dx.doi.org/10.1063/1.4739262
View Table of Contents: http://jap.aip.org/resource/1/JAPIAU/v112/i2
Published by the American Institute of Physics.

Related Articles

Ni59.0Mn23.5In17.5 Heusler alloy as the core of glass-coated microwires: Magnetic properties and magnetocaloric effect
J. Appl. Phys. 112, 033905 (2012)

Critical behavior and magnetocaloric effect of Gd65Mn35−xGex (x=0, 5, and 10) melt-spun ribbons
J. Appl. Phys. 112, 033903 (2012)

Controllable spin-glass behavior and large magnetocaloric effect in Gd-Ni-Al bulk metallic glasses
Appl. Phys. Lett. 101, 032405 (2012)

History dependence of directly observed magnetocaloric effects in (Mn, Fe)As
Appl. Phys. Lett. 100, 252409 (2012)

The magnetocaloric effect of partially crystalline Fe-B-Cr-Gd alloys
J. Appl. Phys. 111, 113919 (2012)

Additional information on J. Appl. Phys.

Journal Homepage: http://jap.aip.org/
Journal Information: http://jap.aip.org/about/about_the_journal
Top downloads: http://jap.aip.org/features/most_downloaded
Information for Authors: http://jap.aip.org/authors

ADVERTISEMENT

Magnetocaloric and transport study of poly- and nanocrystalline composite manganites $La_{0.7}Ca_{0.3}MnO_3/La_{0.8}Sr_{0.2}MnO_3$

M. Pękała,[1,a)] K. Pękała,[2] V. Drozd,[3] K. Staszkiewicz,[1,4] J.-F. Fagnard,[5] and P. Vanderbemden[5]
[1]*Department of Chemistry, University of Warsaw, Al. Zwirki i Wigury 101, PL-02-089 Warsaw, Poland*
[2]*Faculty of Physics, Warsaw Technical University, 00-662 Warsaw, Poland*
[3]*Center for the Study Matter at Extreme Conditions, Florida International University, Miami, Florida 33199, USA*
[4]*College of Inter-Faculty Individual Studies in Mathematics and Natural Sciences, University of Warsaw, Poland*
[5]*SUPRATECS, Department of Electrical Engineering and Computer Science (B28), University of Liège, Belgium*

(Received 4 January 2012; accepted 27 June 2012; published online 24 July 2012)

Magnetocaloric and transport properties are reported for novel poly- and nanocrystalline double composite manganites, $La_{0.8}Sr_{0.2}MnO_3/La_{0.7}Ca_{0.3}MnO_3$, prepared by the sol-gel method. Magnetic field dependence of magnetic entropy change is found to be stronger for the nano- than the polycrystalline composite. The remarkable broadening of the temperature interval, where the magnetocaloric effect occurs in poly- and nanocrystalline composites, causes the relative cooling power (RCP(S)) of the nanocrystalline composite to be reduced by only 10% compared to the Sr based polycrystalline phase. The RCP(S) of the polycrystalline composite becomes remarkably enhanced. The low temperature magnetoresistance is enhanced by 5% for the nanostructured composite. © *2012 American Institute of Physics*. [http://dx.doi.org/10.1063/1.4739262]

INTRODUCTION

Recently, considerable effort has been made to study and modify the magnetocaloric and magneto-transport properties of mixed valence manganites. The scientific interest in these materials is stimulated by the potential applications in magnetic refrigeration as well as in magnetoresistive sensors and transducers.[1,2] Research on magnetic refrigeration is increasing since it may offer higher efficiency than traditional gas compression devices. Moreover, magnetic refrigeration may be more environmentally friendly. There is a search for new materials with a large change in magnetic entropy close to room temperature, which may compete with the expensive gadolinium and its compounds. The doped perovskite manganites are potential candidates due to their high magnetization and Curie temperatures as well as their chemical stability, easy preparation, and relatively low cost.[1]

The cooling power of magnetic refrigeration is controlled both by the magnetic entropy change and the width of the temperature interval, where the magnetocaloric effect appears. A remarkable increase in the width of the temperature interval was reported for nanostructured materials.[3–8]

On the other hand, sensitivity of the electrical resistivity to the magnetic field and a colossal magnetoresistance (MR) are important for the sensor applications. Beyond different types of chemical substitution and treatment processes, the barocaloric effect was also studied.[9] In another approach, materials' properties are changed by creating the composites containing manganites on one side and various secondary magnetic, metallic, insulating, or ferroelectric components on the other.[10–12] The data analysis becomes more complicated when composites contain "foreign" elements since high temperature sintering may enhance the diffusion of such foreign atoms into a manganite phase. This may in turn change the composition and properties of a manganite phase compared to a pristine one. Previous investigation of the manganite/manganite composites is lacking and focuses mainly on magnetoresistance, e.g., Refs. 11 and 12.

The aim of this paper is to study how magnetocaloric and magneto-transport properties of a novel composite containing the two "complementary" orthorhombic $La_{0.7}Ca_{0.3}MnO_3$ and rhombohedral $La_{0.8}Sr_{0.2}MnO_3$ manganites may be modified when crystallite sizes are reduced from the micrometer down to the nanometer scale, inducing higher atomic and magnetic disorder. The double manganite composite has the advantage that any influence of foreign elements is excluded. The possibility of using the composite manganite exhibiting a second order phase transition for refrigeration is evaluated, taking into account the magnitude of the magnetocaloric effect and its relative cooling power. The influence of the magnetic field strength on the magnetocaloric effect and cooling power is quantitatively estimated.

SAMPLE PREPARATION

The initial $La_{0.8}Sr_{0.2}MnO_3$ (LSM) and $La_{0.7}Ca_{0.3}MnO_3$ (LCM) manganites were prepared using the citrate sol-gel precursor method.[13] The starting reagents, La_2O_3, $Sr(NO_3)_2$, $CaCO_3$, and $MnCO_3$, were dissolved in diluted nitric acid with continuous stirring and moderated heating. Lanthanum oxide was calcined at 1000 °C for 24 h prior to use to remove hydroxide and carbonate impurities. A gelation agent, monohydrate of citric acid, was added together with ethylene glycol. The molar ratio of metals:citric acid:ethylene glycol was 1:10:10. The obtained solution was evaporated on a hot plate

a)pekala@chem.uw.edu.pl.

until a homogeneous gel-like product formed. Then the gel was decomposed at 300 °C in air.

Nanocrystalline powders were produced by calcination of a sol-gel precursor at 600 °C for 12 h in an air atmosphere. Calcination of the same precursors at 1250 °C for 24 h with intermediate grinding yielded polycrystalline samples.

Samples of $La_{0.8}Sr_{0.2}MnO_3/La_{0.7}Ca_{0.3}MnO_3$ composites were made by calcining 1:1 (by weight) mixtures of nano- and polycrystalline powders for 2 h at 650 and 1250 °C, respectively.

POWDER SYNCHROTRON XRD CHARACTERIZATION

Angle-dispersive synchrotron x-ray diffraction data were obtained at the 16-IDB beamline of Advanced Photon Source (Argonne National Laboratory) using monochromatic x-rays of wavelength 0.398137 Å (calibrated with the CeO_2 standard) and a high-resolution image plate detector (MAR 345). The recorded two-dimensional diffraction images were integrated with FIT2D[14] and analyzed using the Rietveld method with the GSAS-EXPGUI software package.[15,16]

The unit cell parameters of the orthorhombic $La_{0.7}Ca_{0.3}MnO_3$ and rhombohedral $La_{0.8}Sr_{0.2}MnO_3$ manganites were found to be close to previously reported values.[3,17] After sintering, the rhombohedral $La_{0.8}Sr_{0.2}MnO_3$ manganite shrinks both in the poly- and nanocrystaliine composites as revealed by a reduced unit cell volume. In the case of the orthorhombic $La_{0.7}Ca_{0.3}MnO_3$ manganite, one notices a decrease and increase of cell volume for the nano- and polycrystalline composites, respectively. No phases other than $La_{0.7}Ca_{0.3}MnO_3$ and $La_{0.8}Sr_{0.2}MnO_3$ were detected.

Crystallite size of the synthesized manganites was determined by x-ray diffraction peak broadening (Fig. 1) using Scherrer's formula. Lanthanum hexaboride powder of particle size ~2 μm was used to determine the instrumental contribution to the diffraction peak broadening. Results of the crystallite size determination are listed in Table I together with unit cell parameters of individual Ca- and Sr-based manganites and composites.

The mean crystallite sizes listed in Table I refer to the initial manganites which were used to prepare the manganite composites. The pairs of Ca- and Sr-based manganites subjected to sintering had similar mean crystallite sizes of ~26 to ~29 nm and ~110 to ~135 nm for the nano- and polycrystalline composites, respectively. The composites were made by a short sintering of the manganites, and the increase in crystallite size is estimated to be less than 10%. A direct size determination for the composites was impossible since the diffraction peaks of $La_{0.8}Sr_{0.2}MnO_3$ and $La_{0.7}Ca_{0.3}MnO_3$ overlap. Additionally, the short sintering at relatively low temperatures prevents a strong mixing of the Ca- and Sr-based phases due to ion diffusion. Therefore, the separate Ca- and Sr-based phases are retained in the composites.

MAGNETIC MEASUREMENTS

The DC magnetization measurements were performed in a magnetic field of 100 Oe in field cooled (FC) and zero field cooled (ZFC) modes. Magnetization isotherms of up to H = 20 000 Oe have been recorded in the broad temperature interval. The magnetic and resistivity measurements are described separately in Ref. 18.

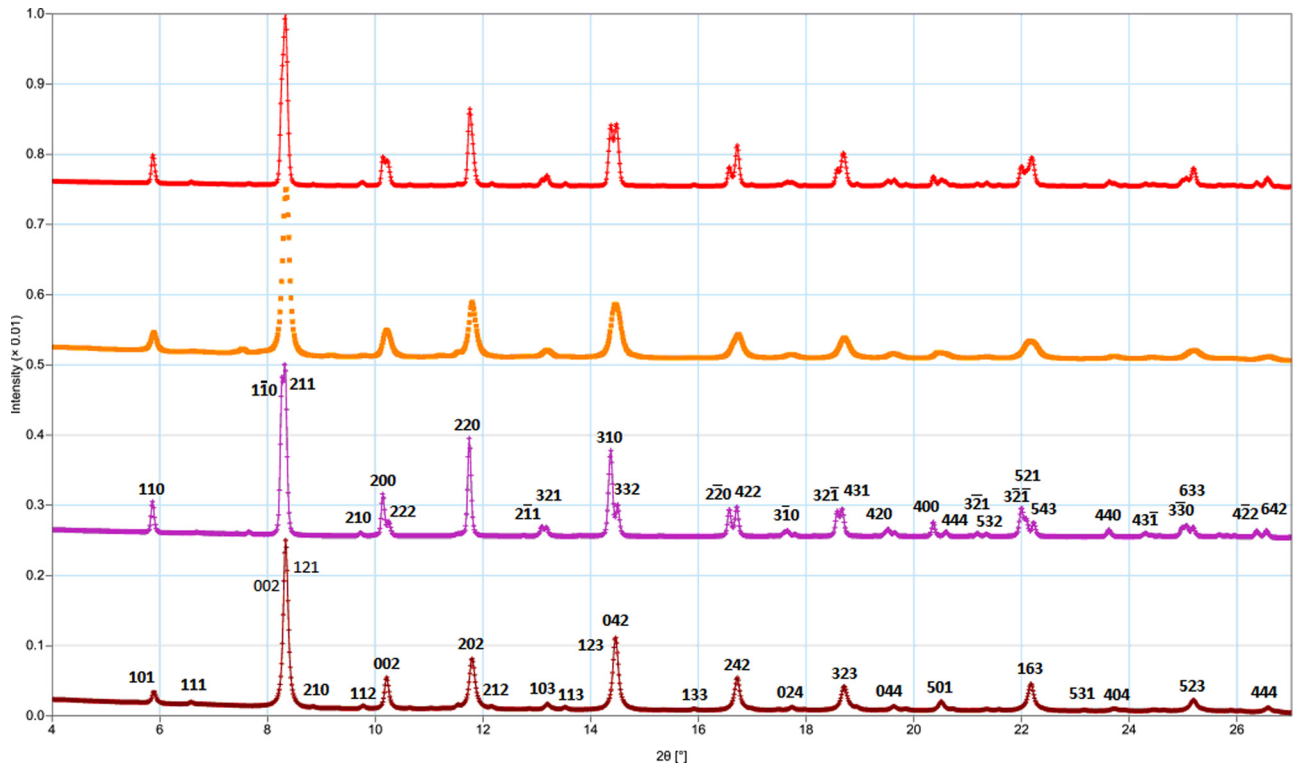

FIG. 1. Synchrotron ($\lambda = 0.398137$ Å) powder XRD patterns (from top to bottom) of polycrystalline LSM-LCM, nanocrystalline LSM-LCM, polycrystalline LSM, and polycrystalline LCM systems.

TABLE I. Crystal lattice parameters for nano- and polycrystalline $La_{0.8}Sr_{0.2}MnO_3$, $La_{0.7}Ca_{0.3}MnO_3$ manganites, and composites.

		R-3c			*Pnma*			
Sample	Average crystallite size, nm	$a=b=c$, Å	$\alpha=\beta=\gamma$, deg	V, Å^3	a, Å	b, Å	c, Å	V, Å^3
Nano-$La_{0.8}Sr_{0.2}MnO_3$	26	5.4800(5)	60.535(6)	117.76(1)				
Poly-$La_{0.8}Sr_{0.2}MnO_3$	110	5.4804(2)	60.539(1)	117.806(6)				
Nano-$La_{0.7}Ca_{0.3}MnO_3$	29				5.4478(8)	7.7602(9)	5.4784(7)	231.6(1)
Poly-$La_{0.7}Ca_{0.3}MnO_3$	135				5.449(1)	7.7611(7)	5.4793(5)	231.73(6)
Nano-composite (1:1 wt. ratio)		5.4703(7)	60.376(7)	116.73(3)	5.418(1)	7.731(2)	5.472(1)	229.2(1)
Poly-composite (1:1 wt. ratio)		5.4796(8)	60.532(7)	117.74(3)	5.476(5)	7.743(6)	5.478(5)	232.3(3)

LOW FIELD MAGNETIZATION

The temperature variation of the FC and ZFC magnetizations exhibits remarkably different behaviors for the poly- and nanocrystalline manganite composites studied (Fig. 2(a)). The magnetization of the nanocrystalline composite is lower than the polycrystalline one. This magnetization suppression is due to a higher amount of magnetic disorder in the nanostructured composite. This is accounted for with a model considering the inner core of grains with magnetization close to that of the bulk material. The outer shell/surface layer is atomically disordered, which in turn depletes its magnetization. The fraction and role of the surface layer increases as the surface to volume ratio increases. As this happens, the grain/crystallite sizes approach the nanometer range.

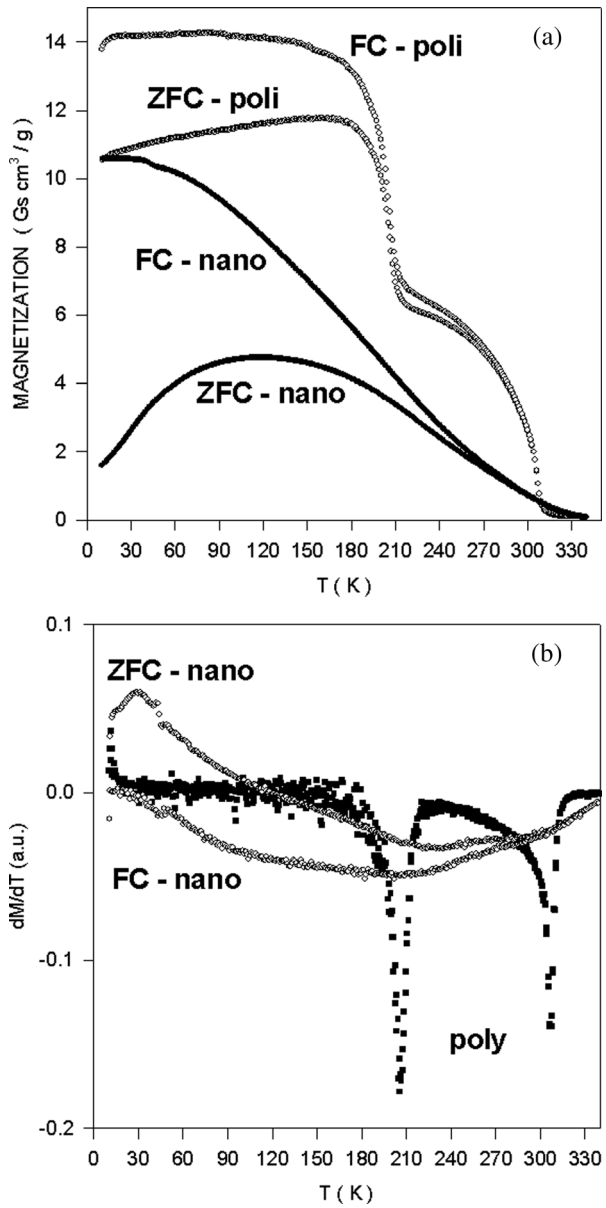

FIG. 2. Temperature variation of the ZFC and FC magnetizations of the poly- and nanocrystalline composites (a). Temperature derivative of the magnetization for the poly- and nanocrystalline composites (b).

The FC and ZFC curves split below the irreversibility temperature at approximately 270 K. The positive slope (dM_{ZFC}/dT) observed below 100 K in the nanocrystalline composite reveals a remarkable contribution from competing antiferromagnetic ordering. In the polycrystalline composite, this contribution is vastly reduced. The thermomagnetic curves with two abrupt drops in magnetization show that the polycrystalline composite contains two phases. The Curie temperatures determined from minimum of the derivative (dM/dT) are equal to 205 and 306 K for the polycrystalline $La_{0.7}Ca_{0.3}MnO_3$ and $La_{0.8}Sr_{0.2}MnO_3$ phases, respectively (Fig. 2(b)). For the nanocrystalline composite, the $M_{FC}(T)$ curve is a smoothly decreasing function. The derivative $dM_{FC}(T)/dT$ has a broad and shallow minimum, which may be related to the broad distribution of local ferromagnetic Curie temperatures.

MAGNETIZATION ISOTHERMS

Magnetization isotherms M(T) were registered in broad temperature intervals: 150 to 336 K for the polycrystalline and 50 to 335 K for the nanocrystalline composites (Fig. 3). They are characteristic for ferromagnetic materials. The polycrystalline low temperature isotherms almost saturate for fields above 4 kOe. On the other hand, the considerable slope of the magnetization isotherms observed in the nanocrystalline composite shows that saturation is not achieved for fields of 20 kOe. Absolute values of magnetization for the nanocrystalline composite are much reduced compared to the polycrystalline one. Such a difference is due to the higher structural and magnetic disorder in the nanostructured composite, as described above.

For the polycrystalline composite, the temperature variation of spontaneous magnetization confirms the coexistence of two magnetic phases, which is revealed by the characteristic shape of the magnetization curve with a distinct change

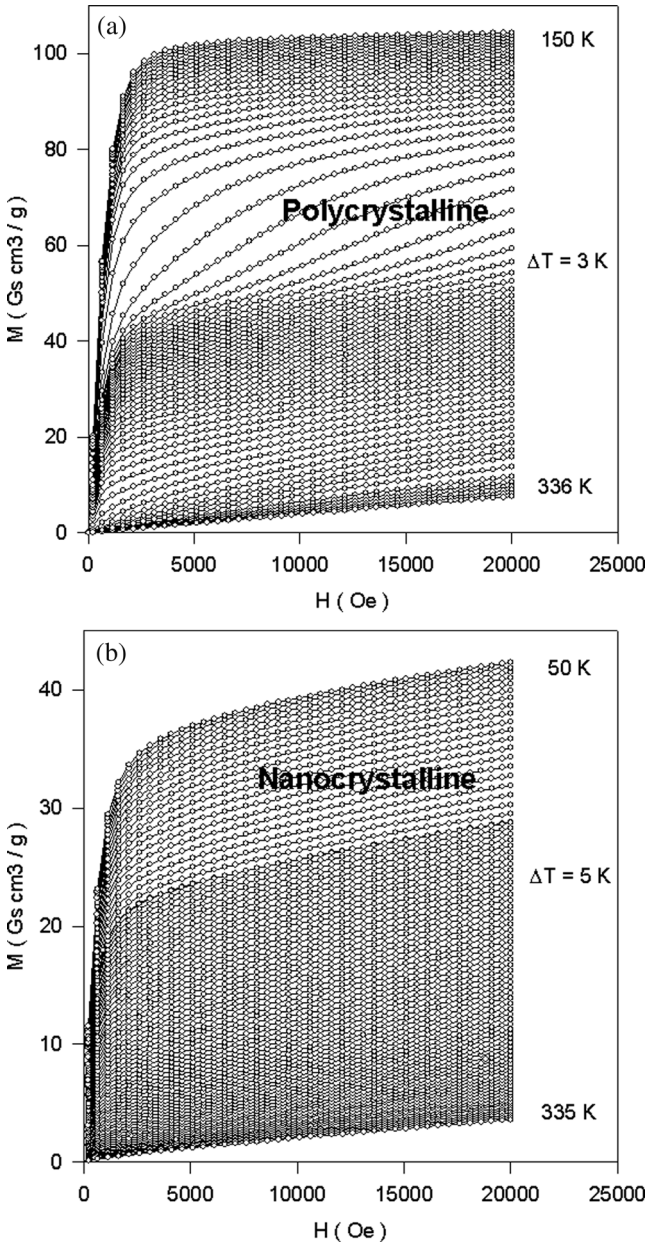

FIG. 3. Magnetization isotherms of the polycrystalline composite for 150–336 K (a) and nanocrystalline composite for 50–335 K (b).

in a slope observed at approximately 220 K (Fig. 4). The low and high temperature ranges correspond to the polycrystalline $La_{0.7}Ca_{0.3}MnO_3$ and $La_{0.8}Sr_{0.2}MnO_3$ phases. A comparison with the FC magnetization at low fields (Fig. 2(a)) shows that the high magnetic field retains the ferromagnetic ordering up to relatively high temperatures of 220 and 315 K for the polycrystalline $La_{0.7}Ca_{0.3}MnO_3$ and $La_{0.8}Sr_{0.2}MnO_3$ phases, respectively. Such a behavior is in contrast to the nanocrystalline composite for which the spontaneous magnetization diminishes almost smoothly in a broad temperature interval.

ARROTT PLOTS

The magnetization isotherms of the poly- and nanocrystalline composites were transformed into Arrott plots which allow the visualization of the following relation:

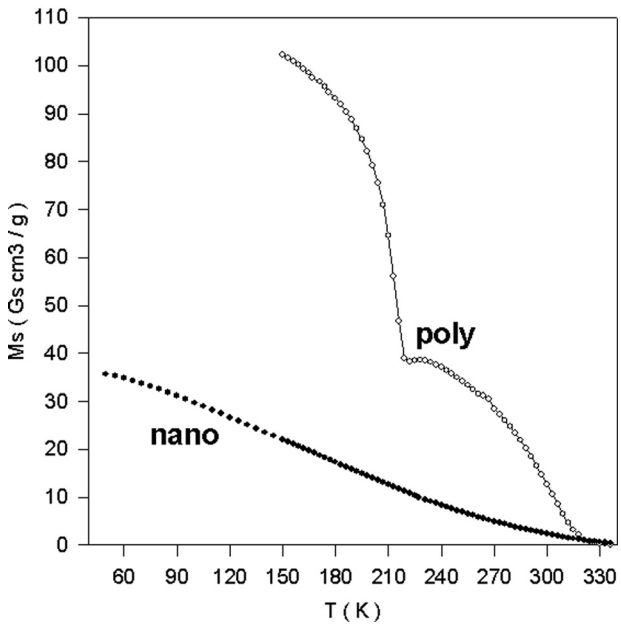

FIG. 4. Temperature variation of spontaneous magnetization for poly- and nanocrystalline composites.

$$A + B\,M^2 = H/M. \quad (1)$$

The thermodynamic A and B parameters correspond to the first coefficients in a power expansion of the thermodynamic potential. A and B are determined by extrapolation of the linear section of the curves appearing in strong magnetic fields.

The positive slope of Arrott plots (Fig. 5) shows that the ferro- to paramagnetic transition is second order for the poly- and nanocrystalline composites. The Curie temperatures are indicated by a sign change of the thermodynamic A parameter (Fig. 6) and are equal to 219 and 294 K for the polycrystalline $La_{0.7}Ca_{0.3}MnO_3$ and $La_{0.8}Sr_{0.2}MnO_3$ phases, respectively. The Curie temperatures derived from the Arrott plots are somewhat different from those found from the low magnetic field magnetization. Such a discrepancy in the Curie temperature confirms the double phase nature of the polycrystalline composite. The above listed Curie temperatures offer only approximate values since a superposition of magnetizations originating from both magnetic phases hinders an analysis. For the nanocrystalline composite, the Curie temperature is about 197 K. This may be regarded as a mean value of the broad distribution of local Curie temperatures in the structurally and magnetically disordered nanocrystalline composite.

MAGNETOCALORIC EFFECT

The magnetic entropy change was derived from magnetization isotherms following the method described previously.[19,20] Temperature variation of the magnetic entropy change (DS(T)) exhibits a distinct behavior for the poly- and nanocrystalline composites (Fig. 7). The DS(T) dependence for a polycrystalline composite has two peaks at 210 and 305 K resembling the DS maxima observed in the parent manganites $La_{0.7}Ca_{0.3}MnO_3$ and $La_{0.8}Sr_{0.2}MnO_3$, respectively.

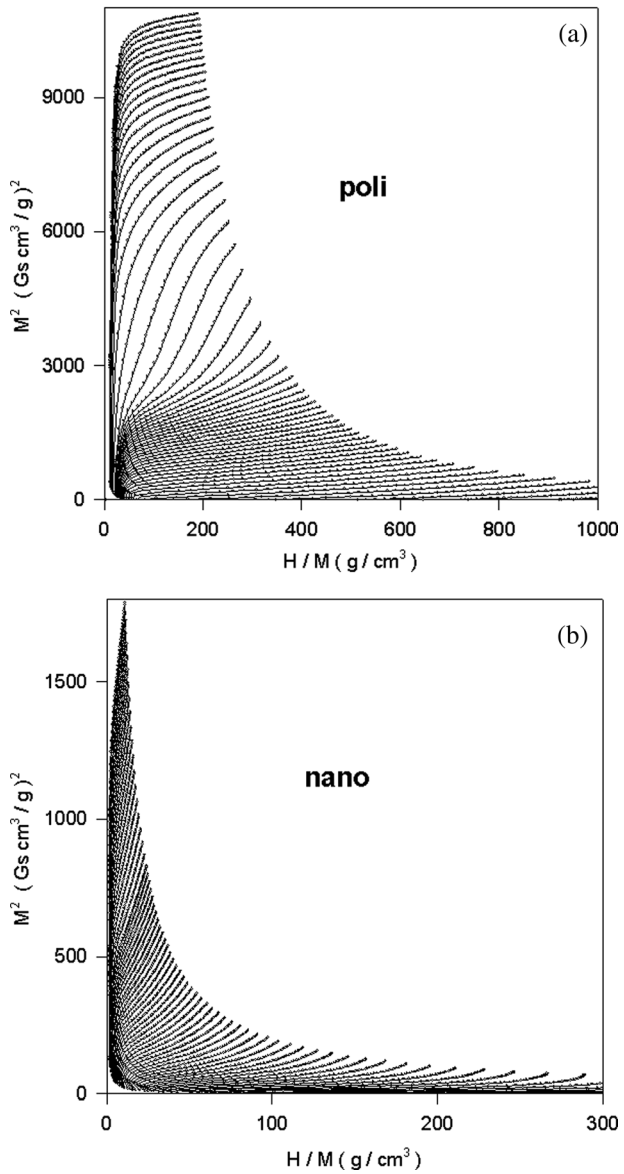

FIG. 5. Arrott plots for the polycrystalline (a) and nanocrystalline (b) composites.

For both DS peaks, the low temperature slope is roughly twice as small as the high temperature slope. This is in contrast to the nanocrystalline composite, where the single, broad, and shallow minimum are found at approximately 180 K. The width of this minimum extends between approximately 60 and 300 K. The DS peaks of the polycrystalline composite are much narrower. It is noteworthy that the temperature width of the nanocrystalline composite is only weakly affected by the magnetic field strength, whereas for the polycrystalline composite, the width increases with the magnetic field. The magnitude of DS in the nanocrystalline composite is several times smaller than for the polycrystalline one. The magnetic field slightly shifts all three DS peaks towards a higher temperature.

The magnetic field dependence of magnetic entropy change is known to vary with temperature, as demonstrated for manganites and metallic alloys.[4,5] This may be accounted for by the empirical formula

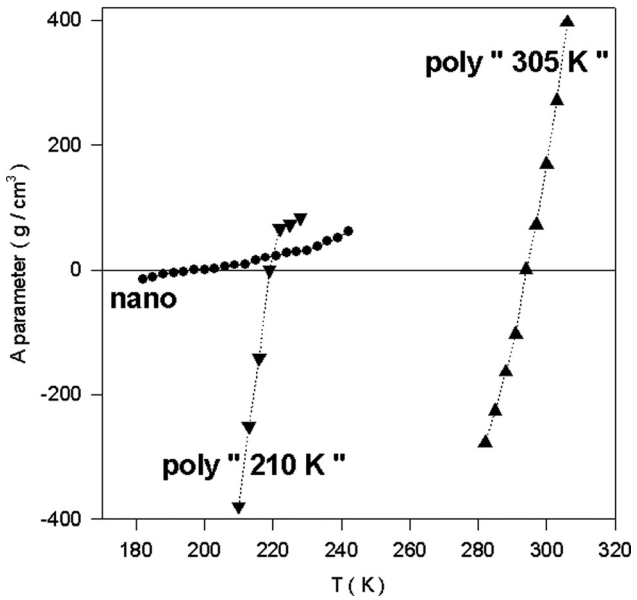

FIG. 6. Temperature variation of the thermodynamic A parameters derived from the Arrott plots for the poly- and nanocrystalline composites.

$$DS(H) = C\,H^{N}, \tag{2}$$

where C is a constant. The N exponent is derived from experimental data of the polycrystalline composite (Fig. 8) and is equal to 0.87 ± 0.06 and 0.99 ± 0.02 for DS peaks at 210 and 305 K, respectively. For the nanocrystalline composite, $N = 1.14 \pm 0.03$. These N values are close to those reported for the $La_{0.7}Ca_{0.3}MnO_3$ and $La_{0.8}Sr_{0.2}MnO_3$ manganites.[4] They confirm the previous observation that the N exponents for nanocrystalline manganites are slightly higher than the polycrystalline ones.[4] This higher N exponent reveals an increased sensitivity of DS of the nanocrystalline composite to magnetic field.

RELATIVE COOLING POWER

The cooling efficiency of a magnetic material is expressed by the relative cooling power (RCP(S)) defined as the product of maximum entropy change DS_M and the DS peak half width DT, $RCP(S) = DS_M{*}DT$. RCP(S) corresponds to the heat transferred by 1 kg of material between temperatures differing by DT. Fig. 9 shows that in magnetic fields up to 2 T the RCP(S) is a monotonically increasing function of field both for the poly- and nanocrystalline composites. Magnetic cooling appears most effective in the vicinity of 305 K for the polycrystalline composite, where a contribution of the $La_{0.8}Sr_{0.2}MnO_3$ phase plays a role between 250 and 320 K and achieves the RCP(S) value of 88 J/kg at 2 T. The RCP(S) of this phase is 2.5 times larger than for pure polycrystalline $La_{0.8}Sr_{0.2}MnO_3$ prepared by the sol-gel method.[21]

The second magnetic transition observed in the polycrystalline composite at 210 K offers an RCP(S) of 51 J/kg within a temperature interval of 25 K. Such RCP(S) is comparable with the value 55 J/kg reported for pure polycrystalline $La_{0.7}Ca_{0.3}MnO_3$ at a 2 T magnetic field.[17]

A more detailed inspection of Fig. 7(a) unveils that in the polycrystalline composite with 1:1 ratio of $La_{0.8}Sr_{0.2}MnO_3$

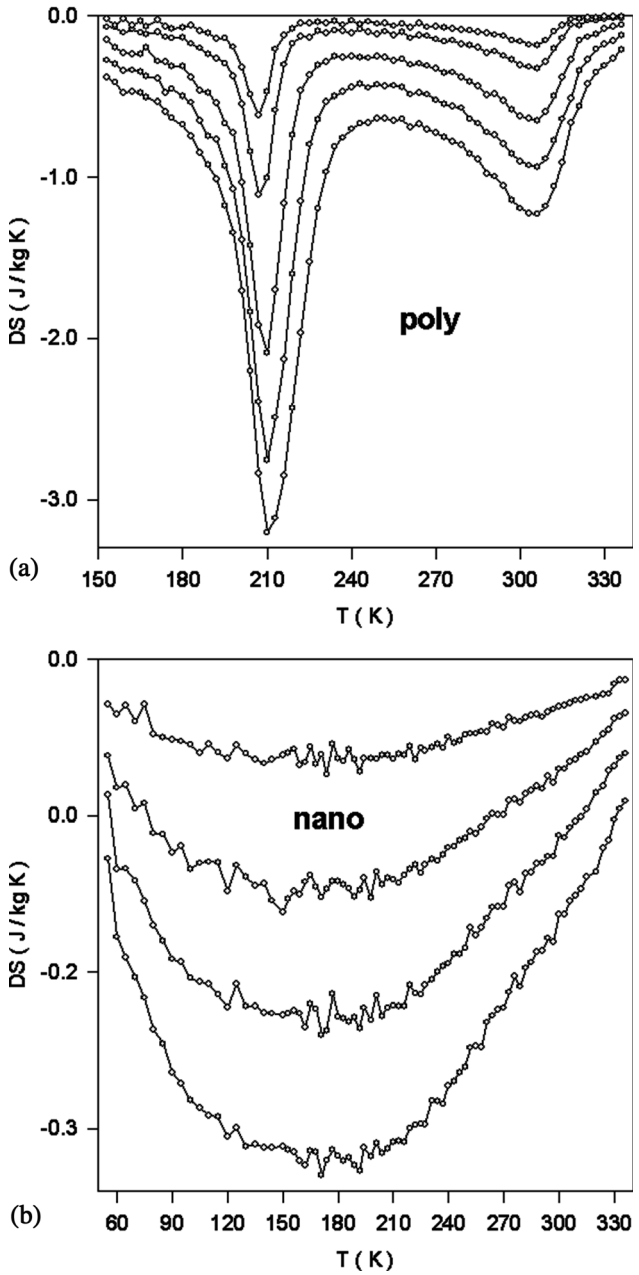

FIG. 7. Temperature variation of the magnetic entropy change for the polycrystalline La(Ca/Sr)MnO_3 composite at a magnetic field change of 0.3, 0.5, 1.0, 1.5, and 2.0 T (from top to bottom) (a) and the nanocrystalline composite La(Ca/Sr)MnO_3 at a magnetic field change of 0.5, 1.0, 1.5, and 2.0 T (from top to bottom) (b).

and $La_{0.7}Ca_{0.3}MnO_3$ phases, the overlapping DS peaks cause a significant broadening of the temperature interval DT. When considering DT at half of the DS peak at 305 K, one finds that DT extends to a very broad range of between 174 and 320 K, which is one of the broadest ranges reported for magnetocaloric materials. Thus, the underestimated RCP, neglecting a contribution from the DS peak at 210 K and taking into account only the maximum magnetic entropy change of the Sr based manganite at 305 K, is equal to 180 J/kg at a magnetic field of 2 T. Such a value competes with the RCP(S) value for Gd of 164 J/kg, interpolated for 2 T.[1]

The RCP(S) of the nanocrystalline composite is also high, achieving 79 J/kg at 2 T in a broad temperature interval

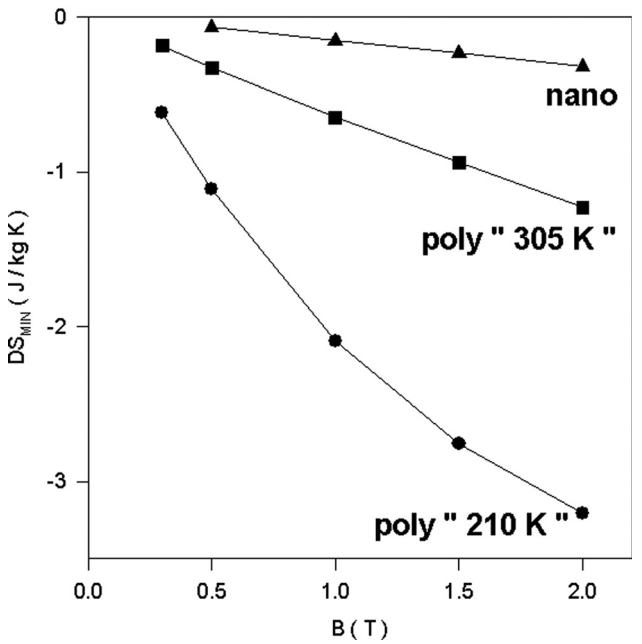

FIG. 8. Magnetic field dependence of the minimum magnetic entropy change for the polycrystalline (a) and nanocrystalline (b) composites.

between 60 and 300 K. RCP(S) of the nanocrystalline composite is more than two times larger than the value for the pure nanocrystalline manganites $La_{0.7}Ca_{0.3}MnO_3$ and $La_{0.8}Sr_{0.2}MnO_3$.[17,21,22]

Recent comparative studies show that a reduction of crystallite sizes during the transition from a poly- to a nanocrystalline composite causes a suppression of magnetic entropy change DS, which is accompanied by a considerable broadening of the temperature interval when compared to the polycrystalline material. Therefore, the cooling power of nanocrystalline composite differs by no more than 10% from that of polycrystalline $La_{0.8}Sr_{0.2}MnO_3$ phase with DS peak at 305 K.

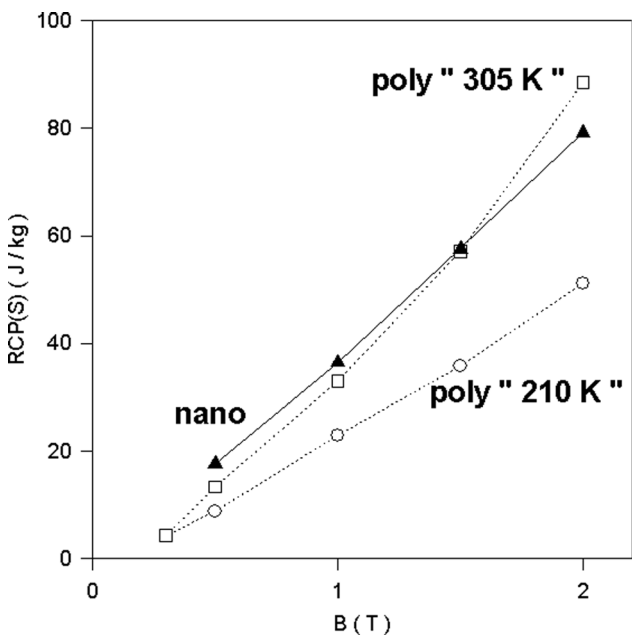

FIG. 9. Magnetic field dependence of RCP(S) for poly- and nanocrystalline composites.

The relative cooling power of RCP(S), being a function of magnetic entropy change magnitude and of temperature width, is known to increase with magnetic field strength. The magnetic field dependence of RCP(S) plotted in Fig. 9 may be approximated by the relation

$$\mathrm{RCP(S)} = \mathrm{D\,H^R}, \tag{3}$$

where D is a constant. Values of the R exponent for the polycrystalline composite are equal to 1.30 ± 0.03 and 1.53 ± 0.09 for DS peaks at approximately 210 and 305 K, respectively. A relatively weaker magnetic field dependence is found for the nanocrystalline composite, where $\mathrm{R} = 1.08 \pm 0.01$.

ELECTRICAL RESISTIVITY AND MAGNETORESISTANCE

At room temperature, the electrical resistivity of the composites (Fig. 10) is of the order of 0.06 and 0.08 Ωm for the poly- and nanocrystalline samples, respectively. Due to shape irregularity, the absolute electrical resistivity is determined with 10% accuracy. The resistivity at 20 K is approximately equal to 0.13 and 1.9 Ωm for the poly- and nanocrystalline composites, respectively. It is worth noting that the resistivity minimum at 38 K is found only for the nanocrystalline composite and shifts slightly with magnetic field varying from zero to 1 T. This minimum reveals the spin dependent charge carrier tunneling/scattering on grain boundaries between antiferromagnetically coupled grains. This resistivity minimum correlates with the antiferromagnetic exchange seen in the ZFC magnetization of the nanocrystalline composite in Fig. 2(a).

The resistivity of the polycrystalline composite achieves a maximum at 162 K which then shifts to 166 K when the magnetic field increases from 0 to 1 T. A similar shift from 112 to 117 K is observed for the nanocrystalline composite. Below the resistivity maximum, the electrical resistivity is of the metallic type, with positive temperature coefficient of resistivity, $\mathrm{dR(T)/dT} > 0$.

The temperature variation of the electrical resistivity in the metallic phase can often be approximated by an exponential expression of the type

$$\rho(\mathrm{T}) = \rho_0 + \mathrm{const\,T^K}, \tag{4}$$

where K is close to 2 and ρ_0 stands for the low temperature residual resistivity. Sometimes even more sophisticated terms with exponents of 4.5 are included and ascribed to the electron-magnon scattering.[23]

The present experimental results cannot be fitted to such a formula since the K exponent rises gradually with temperature from 0.2 up to about 2, just below the resistivity peak for both the poly- and nanocrystalline composites.

In the semiconducting phase, ($\mathrm{d}\rho(\mathrm{T})/\mathrm{dT} < 0$), the electrical resistivity was fitted to various models, including simple thermal activation, adiabatic polaron, bipolaron, nonadiabatic polaron, and variable range hopping. A plausible correlation for each model could be found only in relatively narrow temperature intervals above approximately 220 K. This inapplicability of such approaches which are adequate for single phase materials indicates that the composites studied most likely contain a continuous distribution of grains containing mixed Ca and Sr based phases with a corresponding spectrum of electron transport mechanisms and parameters.

Both the poly- and nanocrystalline composites exhibit a remarkable negative MR effect (Fig. 11). The magnitude of MR defined as

$$\mathrm{MR(T)} = \rho(\mathrm{T,B})/\rho(\mathrm{T},0) - 1, \tag{5}$$

increases with lowering temperature and reaches 31% at 20 K for the polycrystalline composite. MR becomes a

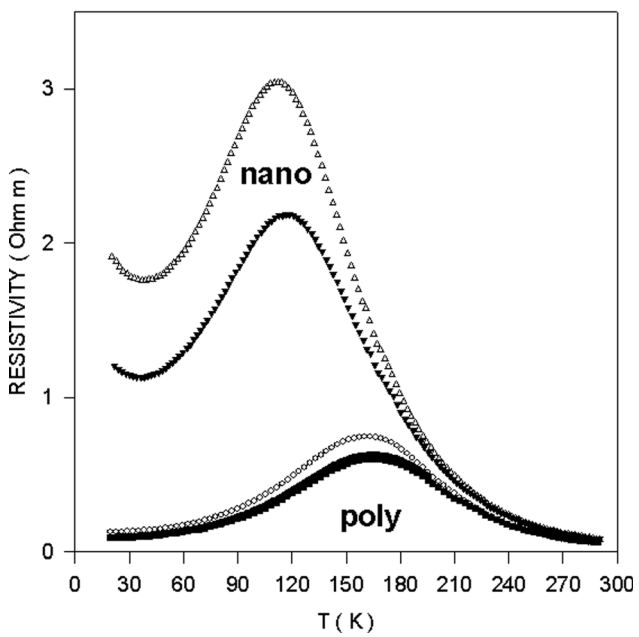

FIG. 10. Temperature variation of electrical resistivity of poly- and nanocrystalline composites in magnetic fields of 0 and 1 T.

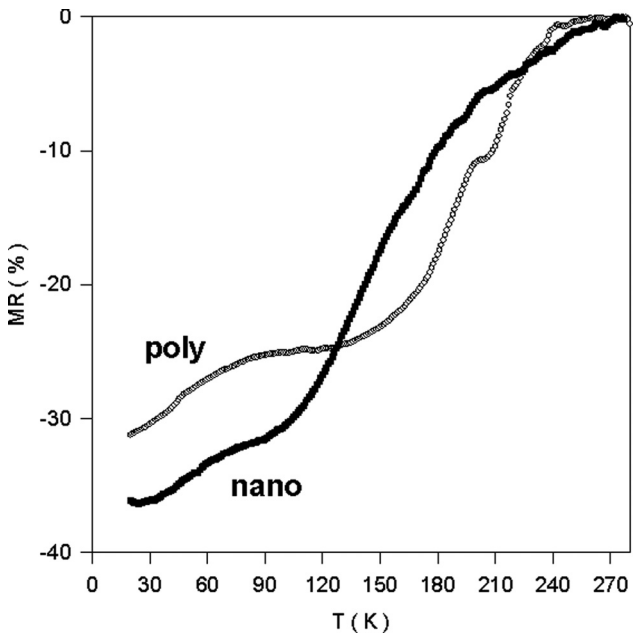

FIG. 11. Temperature variation of the magnetoresistance of poly- and nanocrystalline composites in a 1 T magnetic field.

further 5% stronger for the nanocrystalline composite. Such a variation shows that MR is of the extrinsic type and is caused by spin dependent tunneling between crystallite/grains and/or spin dependent scattering of electrons in the disordered surface layers.[24] These processes are due to the locally changing electronic density which facilitates electron localization. At the lowest temperatures, the sensitivity of magnetoresistance to the magnetic field, defined as dMR/dB, is equal to 31 and 36%/T, which is higher when compared to pure polycrystalline $La_{0.7}Sr_{0.3}Mn_1O_3$[25] and comparable with the composite $La_{0.67}Ca_{0.33}MnO_3/MgO$.[12]

CONCLUSIONS

The collected experimental results show that the composite of two manganites offers an effective way to control and modify the magnetocaloric properties of new materials exhibiting a second order phase transition. In the polycrystalline composite containing equal fractions of $La_{0.8}Sr_{0.2}MnO_3$ and $La_{0.7}Ca_{0.3}MnO_3$ phases, the two separate and overlapping DS peaks cause a significant broadening of temperature interval DT up to 246 K. This results in a large enhancement of relative cooling power to considerably above 180 J/kg at a magnetic field of 2 T. On the transition from the poly- to the nanocrystalline structure, the two partially overlapping peaks of magnetic entropy change are initially well separated at 210 and 305 K, and merge into a broad joint peak at approximately 180 K in the nanocrystalline composite. Two competing processes are observed during this transition. A reduction of crystallite sizes in the composites causes a suppression of the magnetic entropy change. On the other hand, this is accompanied by a broadening of the temperature interval, where a magnetocaloric effect occurs. These processes result in only a 10% reduction in cooling power compared to the DS peak at 305 K of the polycrystalline composite. The relatively high magnetocaloric effect observed in the nanocrystalline composite manganite proves that the structural and magnetic disorder in the outer layers of crystallites is able to broaden the temperature interval. In this scenario, there is no additional broadening contribution due to "foreign" atoms diffusing into outer layer, as observed in composites containing the secondary non-manganite phases. The structural disorder is naturally facilitated by the different orthorhombic and rhombohedral structures of pristine manganites making up the composite. Magnetic entropy change is slightly more sensitive to the magnetic field for the nano- than for the polycrystalline composite. The reverse is found for the cooling power. Magnetocaloric properties of the composites may also be improved by using the proper fraction of components in a composite and by controlling the crystallite sizes during preparation. The magneto-transport properties are also modified by the disordered outer layers leading to a 5% increase of magnetoresistance in the nanocrystalline composite, which leads to a locally percolative like conductivity mechanism.

ACKNOWLEDGMENTS

X-ray diffraction experiments were performed at HPCAT (Sector 16) of the Advanced Photon Source (APS), Argonne National Laboratory. HPCAT is supported by DOE-BES, DOE-NNSA, NSF, and the W.M. Keck Foundation. APS is supported by DOE–BES, under Contract No. DE-AC02-06CH11357. This work performed within the COST MP903 action was supported in part by Ministry of Science and Higher Education (PL) and WBI (B) in a frame of scientific exchange agreement.

[1]M. H. Phan and S. C. Yu, J. Magn. Magn. Mater. **308**, 325 (2007).
[2]Q. Zhang, S. Thota, F. Guillou, P. Padhan, V. Hardy, A. Wahl, and W. Prellier, J. Phys.: Condens. Matter **23**, 052201 (2011).
[3]M. Pękała, N. Kozlova, and V. Drozd, J. Appl. Phys. **104**, 123902 (2008).
[4]M. Pękała, J. Appl. Phys. **108**, 113913 (2010).
[5]V. Franco, C. F. Conde, J. S. Blazquez, A. Conde, P. Svec, D. Janickovic, and L. F. Kiss, J. Appl. Phys. **101**, 093903 (2007).
[6]S. P. Mathews and S. N. Kaul, Appl. Phys. Lett. **98**, 172505 (2011).
[7]A. Biswas, T. Samanta, S. Banerjee, and I. Das, Appl. Phys. Lett. **92**, 212502 (2008).
[8]A. Biswas, T. Samanta, S. Banerjee, and I. Das, J. Appl. Phys. **103**, 013912 (2008).
[9]R. Szymczak, R. Kolano, A. Kolano-Burian, J. Piętosa, and H. Szymczak, J. Magn. Magn. Mater. **322**, 1589 (2010).
[10]M. Triki, R. Dhahri, M. Bekri, E. Dhahri, and M. A. Valente, J. Alloys Compd. **509**, 9460 (2011).
[11]P. T. Phong, N. V. Dai, D. H. Manh, T. D. Thanh, N. V. Khiem, L. V. Hong, and N. X. Phuc, J. Magn. Magn. Mater. **322**, 2737 (2010).
[12]H. Yang, Z. E. Cao, X. Shen, T. Xian, W. J. Feng, J. L. Jiang, Y. C. Feng, Z. Q. Wei, and J. F. Dai, J. Appl. Phys. **106**, 104317 (2011).
[13]M. Gaudon, C. L. Robert, F. Ansart, P. Stevens, and A. Rousset, Solid State Sci. **4**, 125–133 (2002).
[14]A. P. Hammersley, ESRF Internal Report ESRF97HA02T, 1997.
[15]A. C. Larson and R. B. Von Dreele, Los Alamos National Laboratory Report LAUR 86, 2004.
[16]B. H. Toby, J. Appl. Cryst. **34**, 210 (2001).
[17]M. Pękała and V. Drozd, J. Non-Cryst. Solids **354**, 5308 (2008).
[18]M. Pękała, V. Drozd, J. F. Fagnard, Ph. Vanderbemden, and M. Ausloos, J. Appl. Phys. **105**, 013923 (2009).
[19]M. Pękała, V. Drozd, J. F. Fagnard, and Ph. Vanderbemden, J. Alloys Compd. **507**, 350 (2010).
[20]M. Pękała, K. Pękała, V. Drozd, J. F. Fagnard, and P. Vanderbemden, J. Magn. Magn. Mater. **322**, 3460 (2010).
[21]M. Pękała, V. Drozd, J. F. Fagnard, P. Vanderbemden, and M. Ausloos, Appl. Phys. A **90**, 237 (2008).
[22]M. Pękała and V. Drozd, J. Alloys Compd. **456**, 30 (2008).
[23]A. G. Gamzatov, A. B. Batdalov and I. K. Kamilov, Physica B **406**, 2231 (2011).
[24]M. A. Lopez-Quintela, L. E. Huesco, J. Rivas, and F. Rivadulla, Nanotechnology **14**, 212 (2003).
[25]Y. M. Kang, H. J. Kim, and S. I. Yoo, Appl. Phys. Lett. **95**, 052510 (2009).